



Figures and figure supplements

Mechanisms underlying the response of mouse cortical networks to optogenetic manipulation

Alexandre Mahrach et al

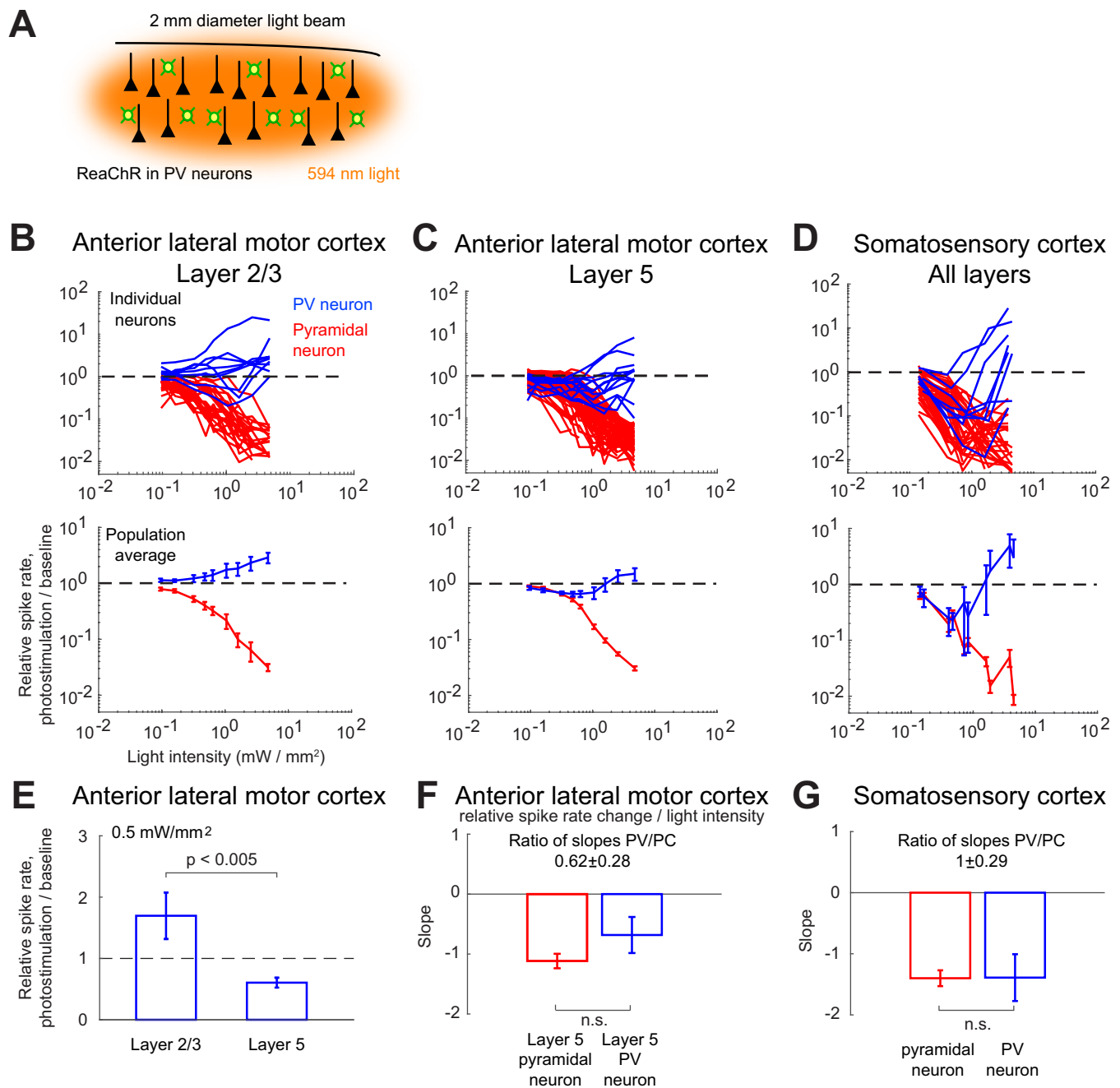


Figure 1. Effects of photostimulation of PV-positive interneurons in the mouse neocortex. (A) Scheme of the experiment. (B–C) Normalized spike rate as a function of laser intensity in different layers and brain areas. Top, individual neuron responses of the PCs (red) and PV (blue) neurons; bottom, population average responses. (B) ALM: layer 2/3: $n = 26$ (PCs), $n = 9$ (PV); (C) ALM layer 5: $n = 62$ (PCs), $n = 12$ (PV). (D) S1: $n = 52$ (PCs), $n = 8$ (PV). Mean \pm s.e.m. across neurons, bootstrap. (E) Comparison of PV neurons' normalized spike rates between ALM Layer 2/3 and Layer five at laser intensity 0.5 mW/mm^2 . (F) Slope of PCs and PVs' normalized spike rate as a function of laser intensity. Data from ALM layer 5. Slopes are computed using data from 0.3 mW/mm^2 and below, before the spike rate of PV neurons begin to increase. Mean \pm SEM, bootstrap (Methods). (G) Same as (F) but for data from S1. In (F and G) the difference between the slopes for the PC and PV populations is not significant.

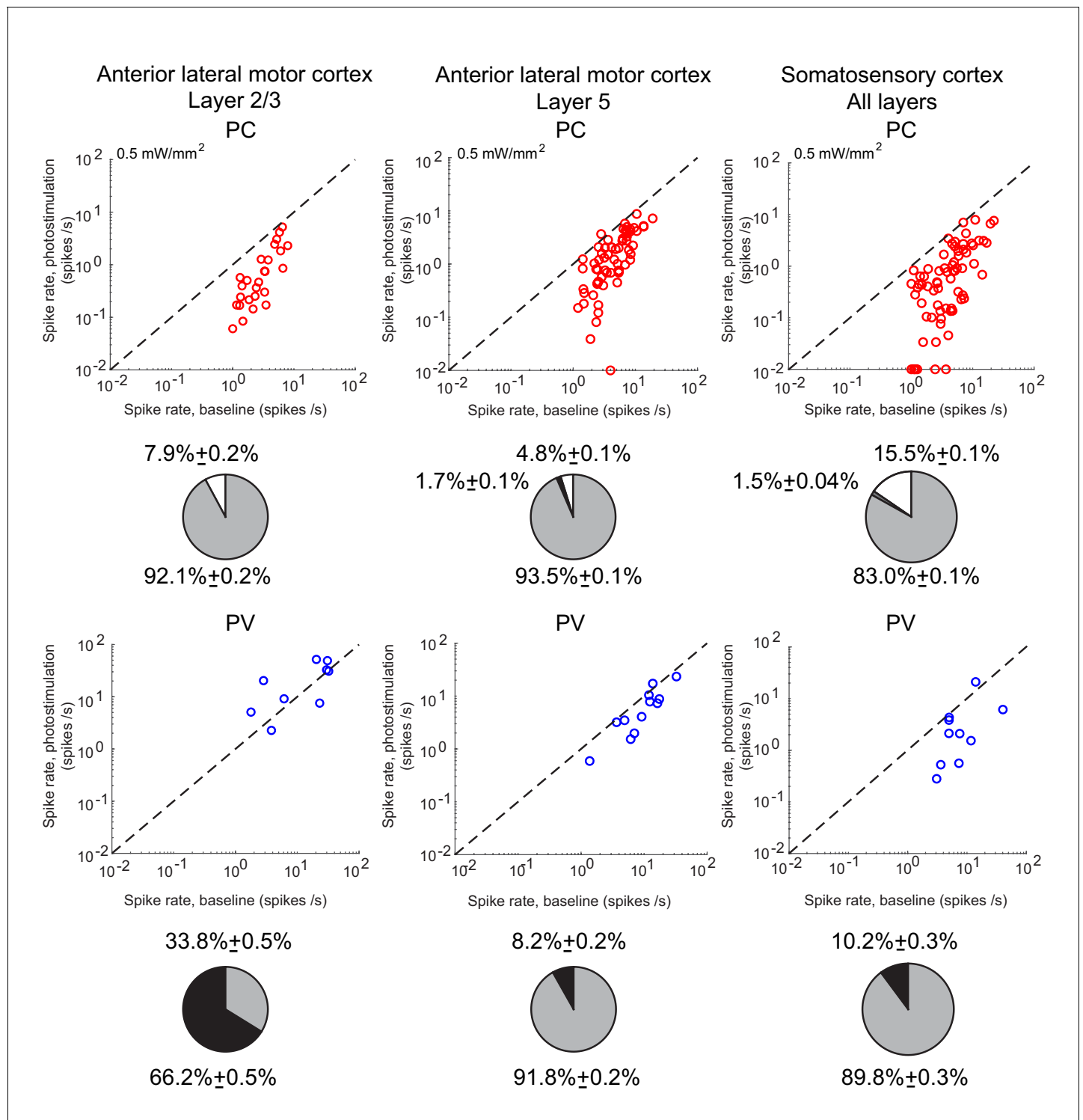


Figure 2. Spike rates of PCs (top) and PV neurons (bottom). Dots correspond to individual neurons. Laser intensity is 0.5 mW/mm². Pie charts represent the fraction of neurons with different types of changes. Mean ± s.e.m. bootstrap. Black, fraction of neurons with activity increase larger than 0.1 Hz. Light gray, fraction of neurons with activity decrease larger than 0.1 Hz. Dark gray, fraction of neurons with activity change smaller than 0.1 Hz. White, fraction of neurons with activity smaller than 0.1 Hz upon PV photostimulation.

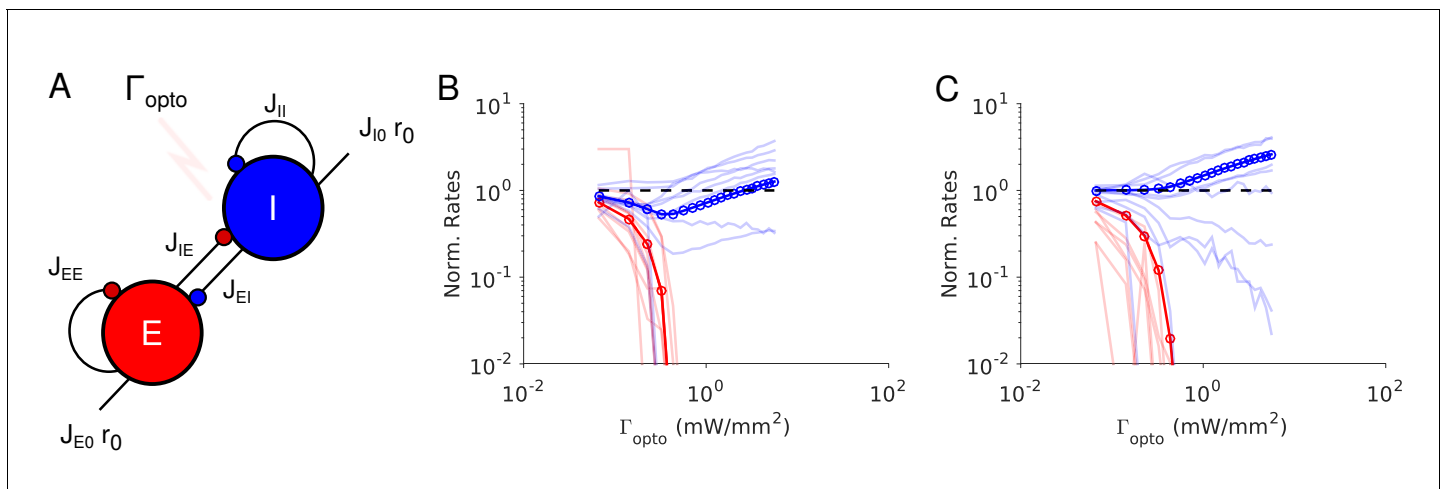


Figure 3. Paradoxical effects in the two-population model. (A) The network. (B–C) Responses of PCs and PV neurons normalized to baseline vs. the laser intensity, Γ_{opto} , for different values of the recurrent excitation, j_{EE} . (B) $j_{EE} = J_{EE} / \sqrt{K}$, the network exhibits the paradoxical effect. (C) $j_{EE} = 0$, the population activity of PV neurons is almost insensitive to small laser intensities. Red: PCs. Blue: PV neurons. Thick lines: population averaged responses. Thin lines: responses of 10 neurons randomly chosen in each population. Firing rates were estimated over 100s. Parameters: $N_E = 57600$, $N_I = 19200$, $K = 500$, $N_I = 19200$. Other parameters as in **Tables 1–2**. Baseline firing rates are: $r_E = 5.7\text{Hz}$, $r_I = 11.7\text{Hz}$ (B) and $r_E = 1.5\text{Hz}$, $r_I = 5.7\text{Hz}$ (C). At the minimum of r_I in (B), $r_E = 0.06\text{Hz}$.

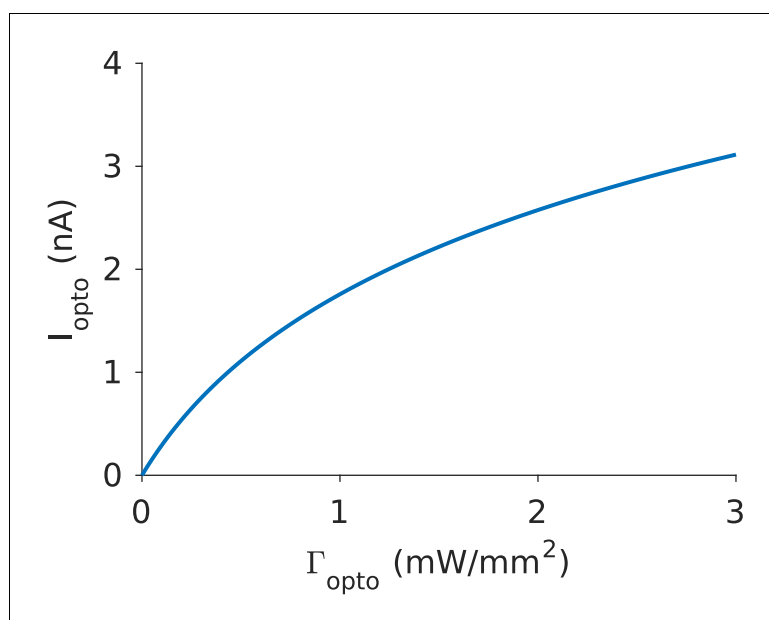


Figure 3—figure supplement 1. Current, I_{opto} , v.s. laser intensity, Γ_{opto} . Parameters are $I_0 = 8\text{ nA}$, $\Gamma_0 = 0.5\text{ mW}\cdot\text{mm}^{-2}$.

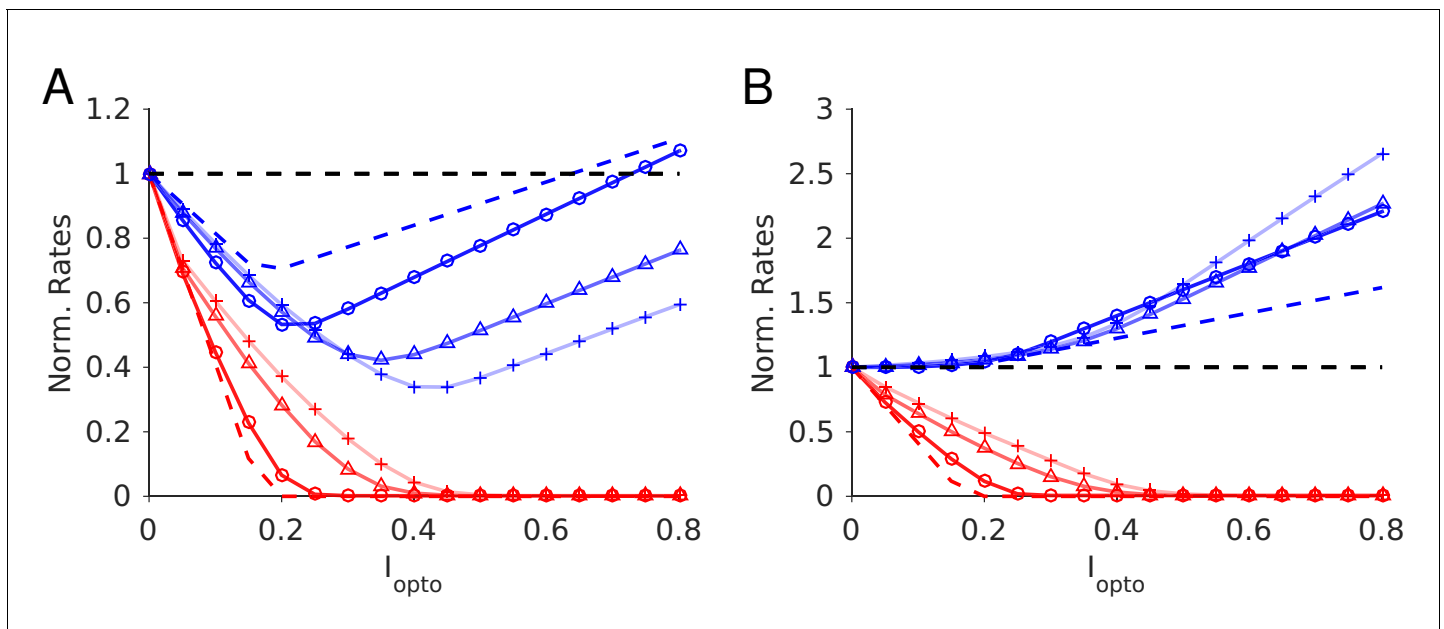


Figure 3—figure supplement 2. Effects of K on the responses of a two-population network to photoactivation of the inhibitory population. (A) $J_{EE} = 22 \mu\text{A.ms.cm}^{-2}$, the inhibitory population activity always recovers when the PCs are silenced. (B) $J_{EE} = 0$, as K increases, the response of the inhibitory population becomes more and more insensitive to the perturbation. Cross: $K = 50$; triangles: $K = 100$; circles: $K = 500$. Dashed line: $\rightarrow \infty$. Color code and parameters as in **Figure 3**. Baseline firing rates: A. $K = 50$: $r_E = 10.8 \text{ Hz}$, $r_I = 16.8 \text{ Hz}$; $K = 100$: $r_E = 8.8 \text{ Hz}$, $r_I = 14.7 \text{ Hz}$; $K = 500$: $r_E = 5.7 \text{ Hz}$, $r_I = 11.7 \text{ Hz}$; $K = \infty$: $r_E = 3.9 \text{ Hz}$, $r_I = 8.5 \text{ Hz}$. B. $K = 500$: $r_E = 1.9 \text{ Hz}$, $r_I = 3.6 \text{ Hz}$; $K = 100$: $r_E = 2 \text{ Hz}$, $r_I = 4.8 \text{ Hz}$; $K = 500$: $r_E = 1.5 \text{ Hz}$, $r_I = 5.7 \text{ Hz}$; $K = \infty$: $r_E = 1.4 \text{ Hz}$, $r_I = 9.1 \text{ Hz}$.

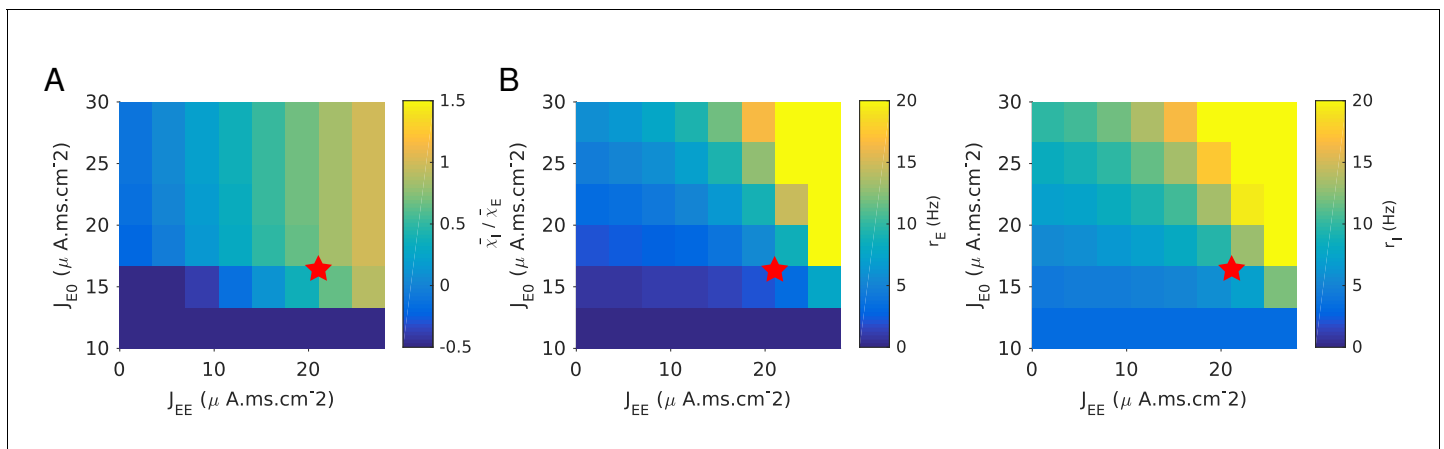


Figure 3—figure supplement 3. Two-population model. The response of the PC and PV populations upon stimulation of the latter are proportional only if parameters are fine-tuned. (A) $\bar{\chi}_I / \bar{\chi}_E$ where $\bar{\chi}_\alpha = (r_\alpha^{lighton} / r_\alpha - 1) / \Gamma_{opto}$ estimated for $\Gamma_{opto} = 0.5 mW.mm^{-2}$. The ratio is close to one only if $J_{EE} \approx J_{EI}J_{IE}/J_{II} = 30 \mu A.ms.cm^{-2}$. (B) Red star indicates the approximate center of the region with proportionality of the responses together with reasonable activities. Parameters as in **Figure 3**. $K = 500$.

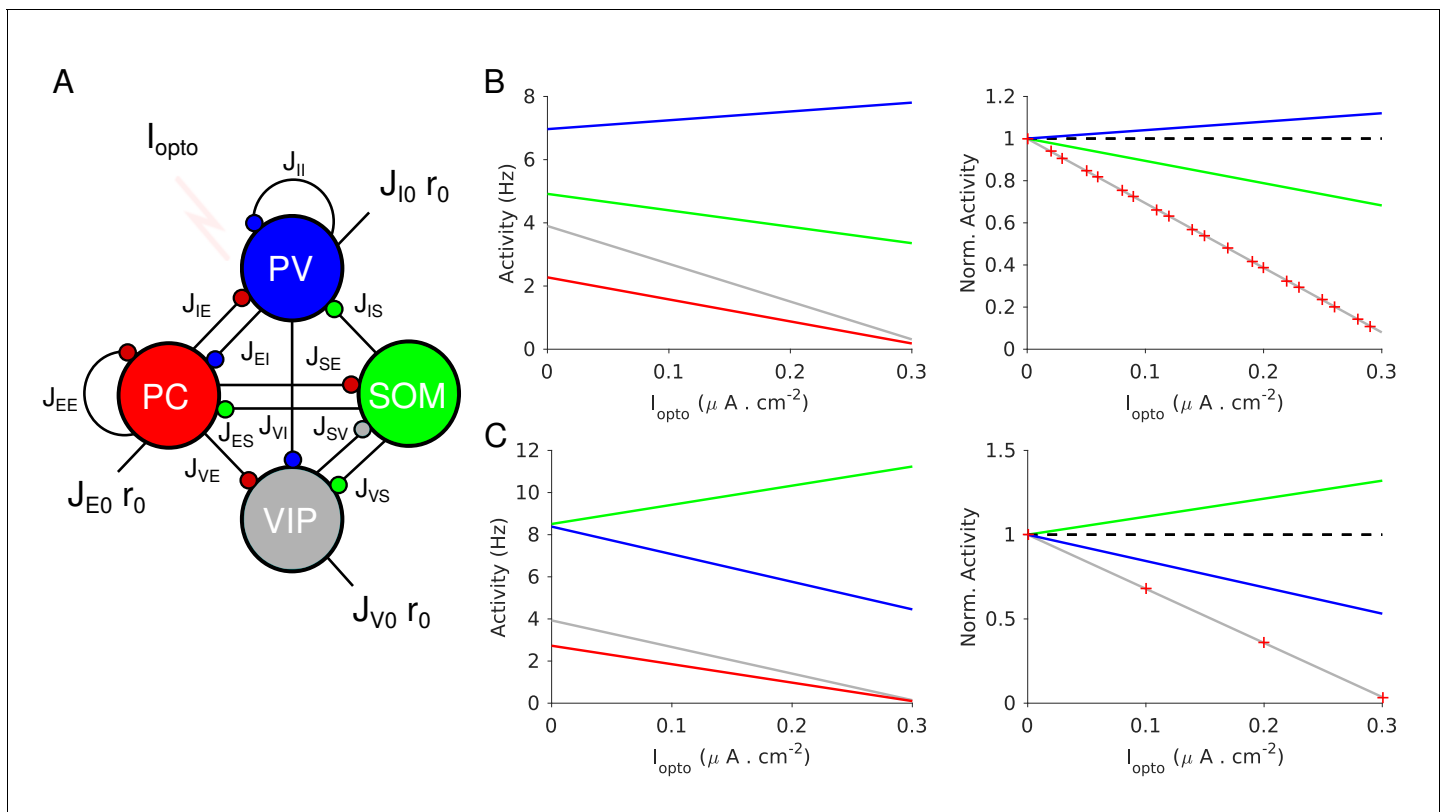


Figure 4. Population activities vs. I_{opto} in Model 1 in the large N, K limit. **(A)** The network is composed of four populations representing PCs, PV, SOM and VIP neurons. The connectivity is as in [Pfeffer et al. \(2013\)](#). **(B)** Parameters as in [Table 4](#). The activity of PV cells increases with I_{opto} while for the three other populations it decreases. **(C)** Parameters as in [Table 5](#). The activity of SOM neurons increases with I_{opto} while for the three other populations it decreases. Right panels in B and C: the activities are normalized to baseline.

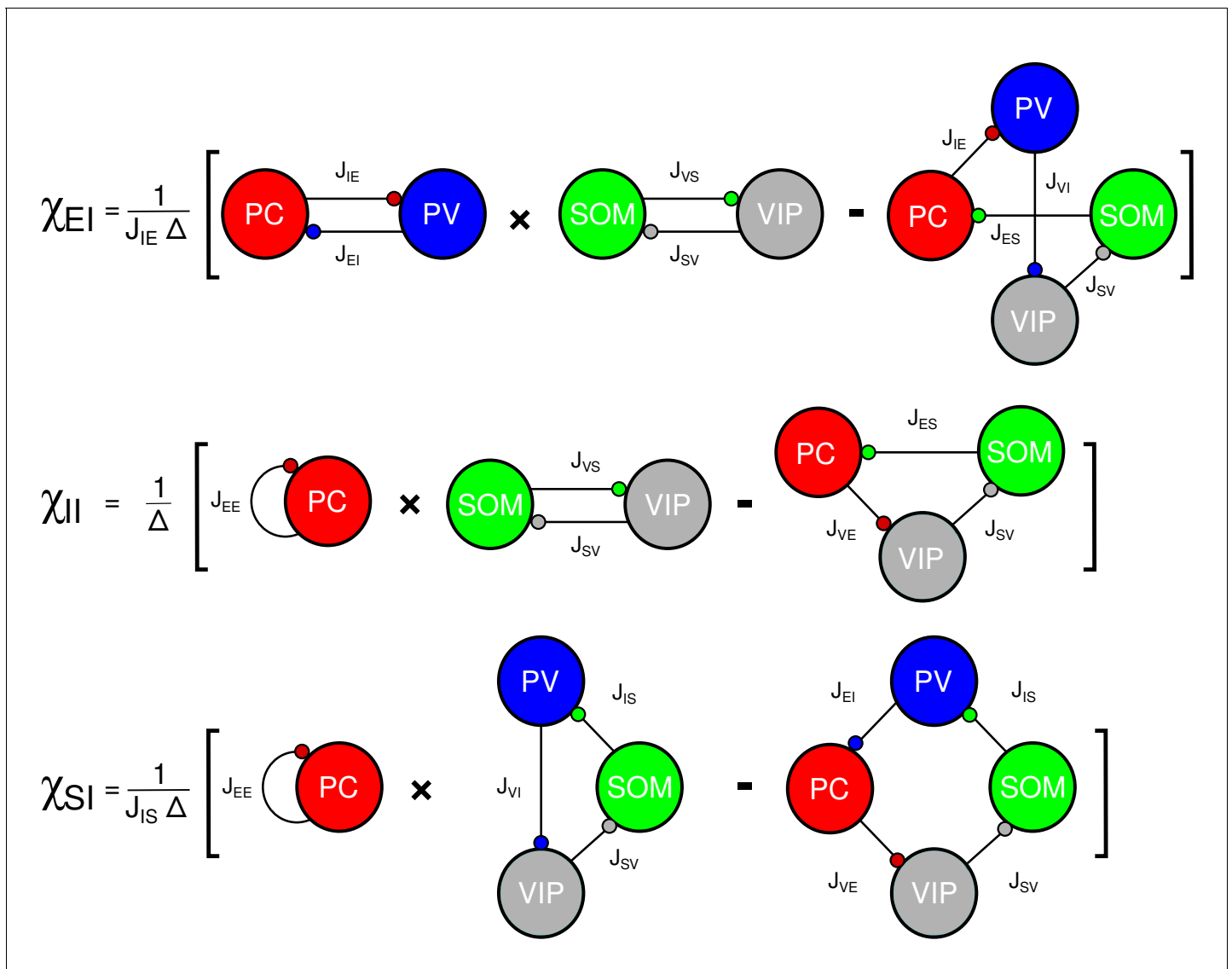


Figure 4—figure supplement 1. Graphical representation of the population susceptibilities upon stimulation of PV in Model 1 (large N , E limit). The prefactor in front of each diagram accounts for the fact that additional terms are needed to complete the loops. Note: $\chi_{VI} = \frac{J_{SE}}{J_{SV}} \chi_{EI}$.

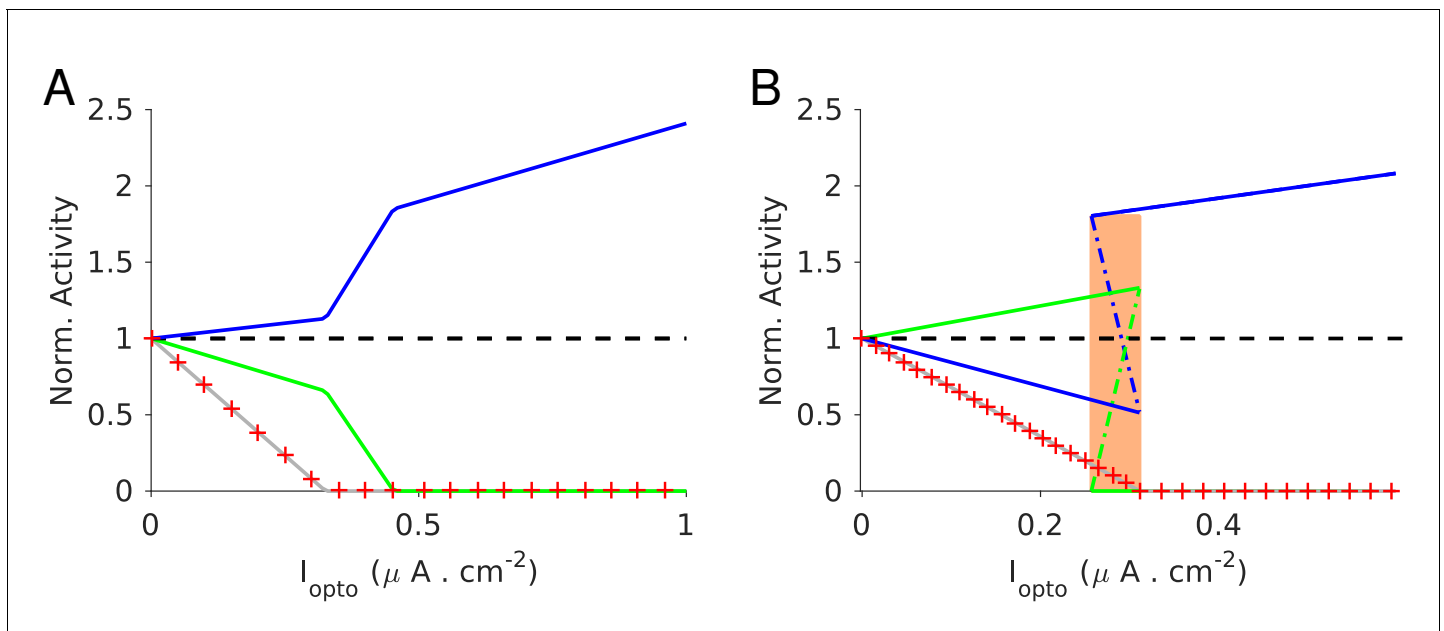


Figure 4—figure supplement 2. Population activities vs. I_{opto} in Model 1 (large N , K limit). The activities are normalized to baseline. **(A)** Parameters as in **Table 4**. The activity of the PV (blue) population increases with I_{opto} . For PC (red cross), SOM (green) and VIP (gray) the activity decreases. **(B)** Parameters as in **Table 5**. In the shaded region, the network is bistable. In one stable state all the four populations are active. In the other stable state, only the PV population is active. A third state in which only the PV and SOM populations are active exists in this range of laser intensity (dotted-dashed line). This state is unstable. Baseline firing rates as in **Figure 4**.

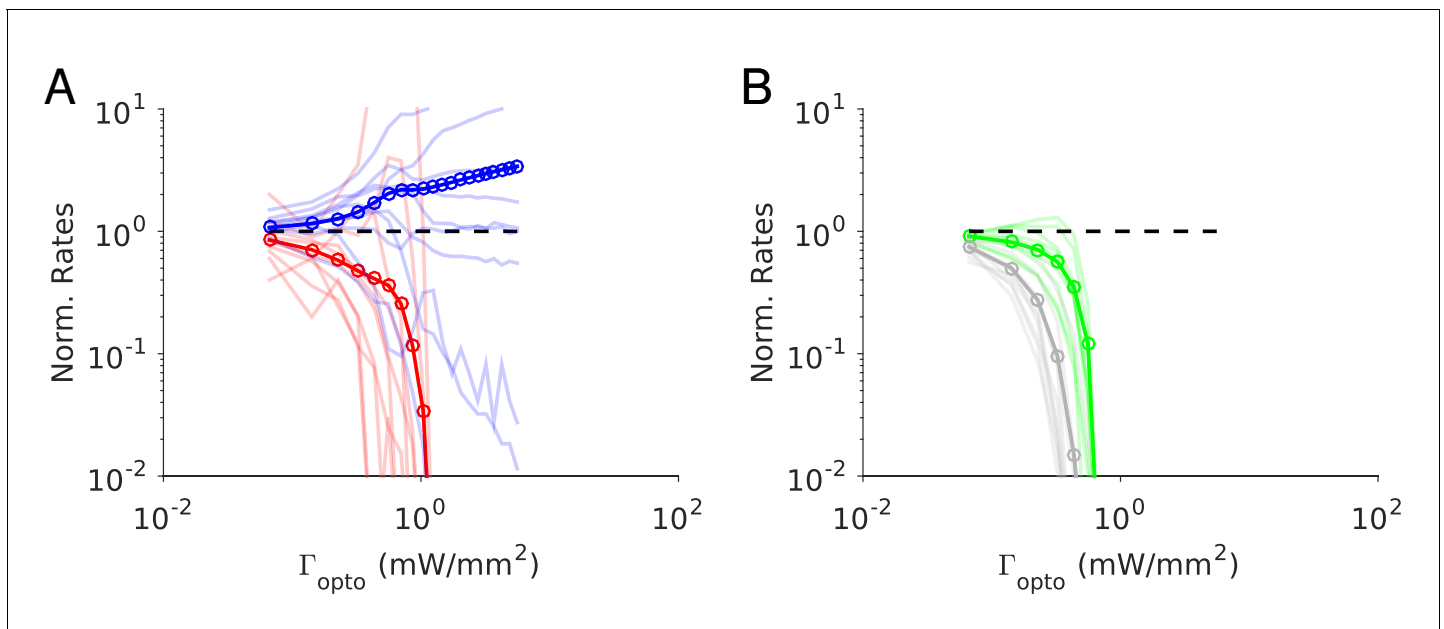


Figure 5. Numerical simulations of Model 1 for $J_{EE} > J_{EE}^*$. Responses of the neurons normalized to baseline vs. the intensity of the laser, Γ_{opto} . (A) Activities of PCs and PV neurons: the PV response is not paradoxical. (B) Activities of SOM and VIP neurons. Color code as in **Figure 4**. Thick lines: population averaged responses. Thin lines: responses of 10 neurons randomly chosen in each population. Firing rates were estimated over 100s. Parameters: $K = 500$, $N = 76800$. Other parameters as in **Tables 3–4**. The baseline activities are: $r_E = 3.3 \text{ Hz}$, $r_I = 6.5 \text{ Hz}$, $r_S = 5.9 \text{ Hz}$, $r_V = 3.5 \text{ Hz}$.

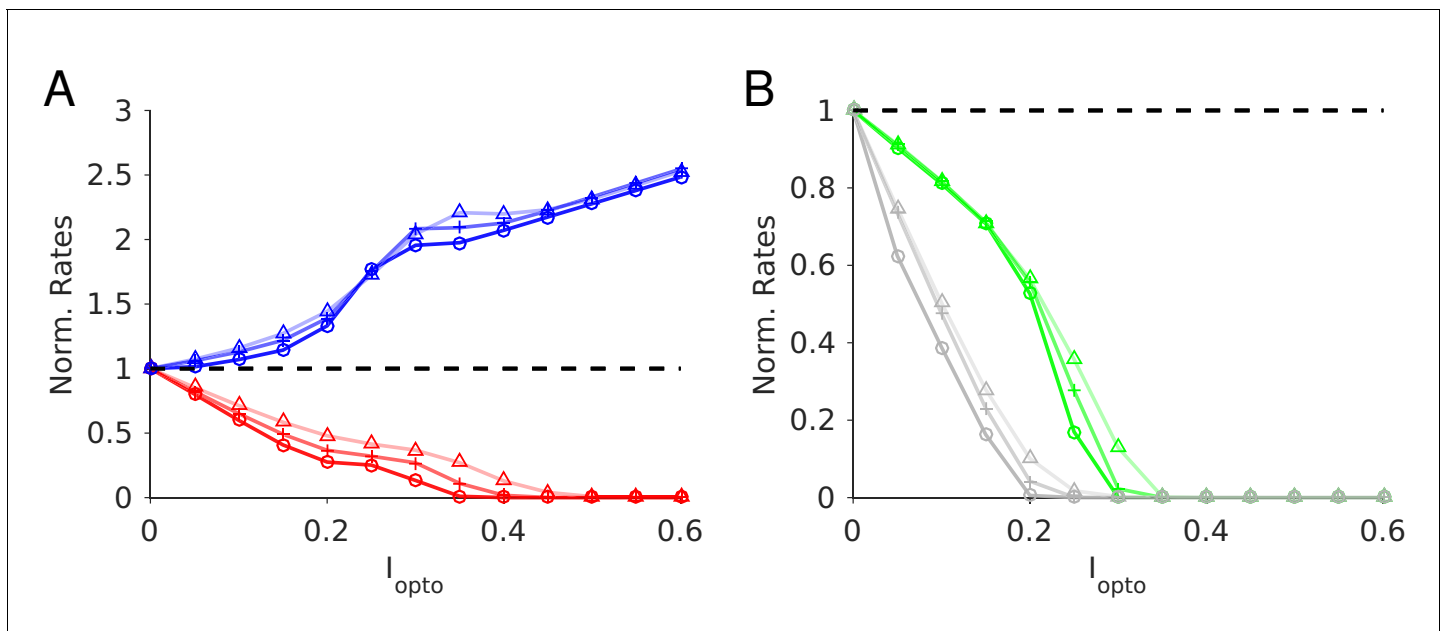


Figure 5—figure supplement 1. Model 1 with $J_{EE} > J_{EE}^*$. Robustness with respect to change in the average connectivity, K . Triangles: $K = 500$; cross: $K = 1000$; circles: $K = 2000$. $N_\alpha = 10000$ neurons per population. Baseline firing rates: $K = 500$: $r_E = 3.3$ Hz, $r_I = 6.5$ Hz, $r_S = 5.9$ Hz, $r_V = 3.5$ Hz; $K = 1000$: $r_E = 3.0$ Hz, $r_I = 6.6$ Hz, $r_S = 5.6$ Hz, $r_V = 3.7$ Hz; $K = 2000$: $r_E = 2.9$ Hz, $r_I = 6.7$ Hz, $r_S = 5.4$ Hz, $r_V = 3.8$ Hz. Rates are averaged over 10s. Color code and parameters as in **Figure 5**.

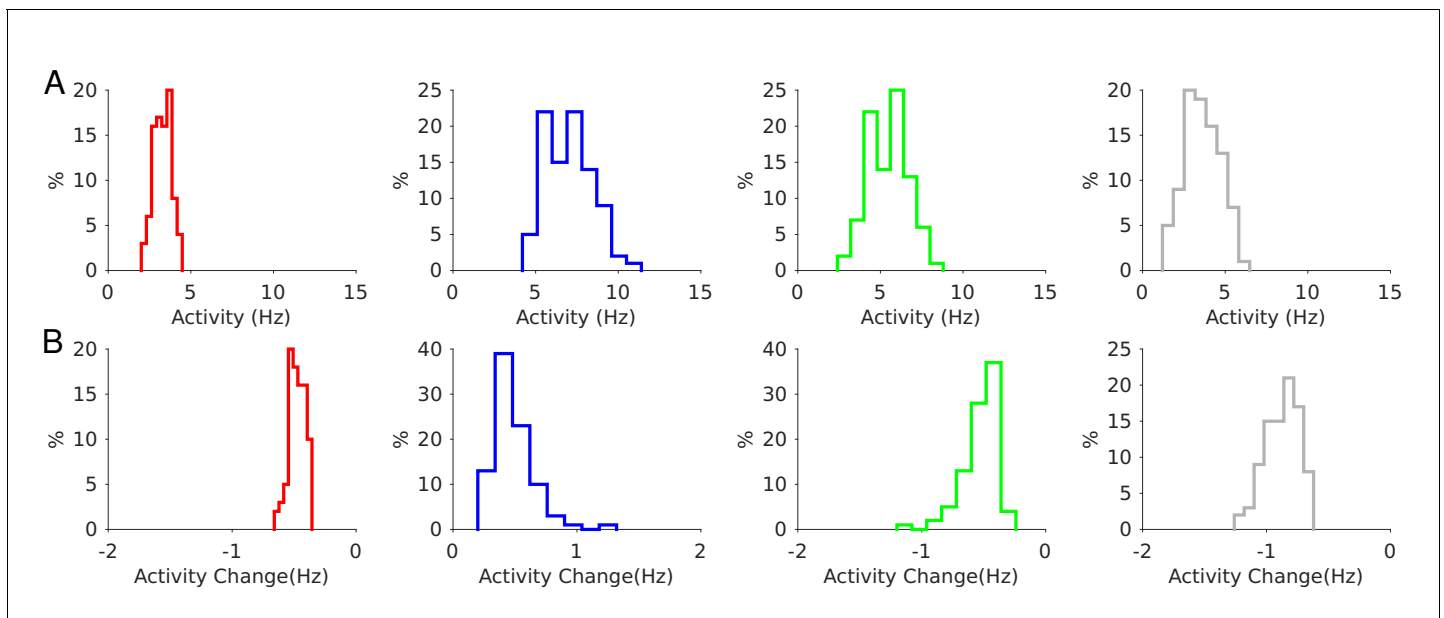


Figure 5—figure supplement 2. Model 1 with $J_{EE} > J_{EE}^*$. Robustness to a change of $\pm 10\%$ in the interaction parameters. (A) Distribution of the population activities. (B) Distribution of the activity changes upon stimulation for $\Gamma_{opto} = 0.07 mW.mm^{-2}$. Color code as in **Figure 5**. Rates are averaged over 10s.

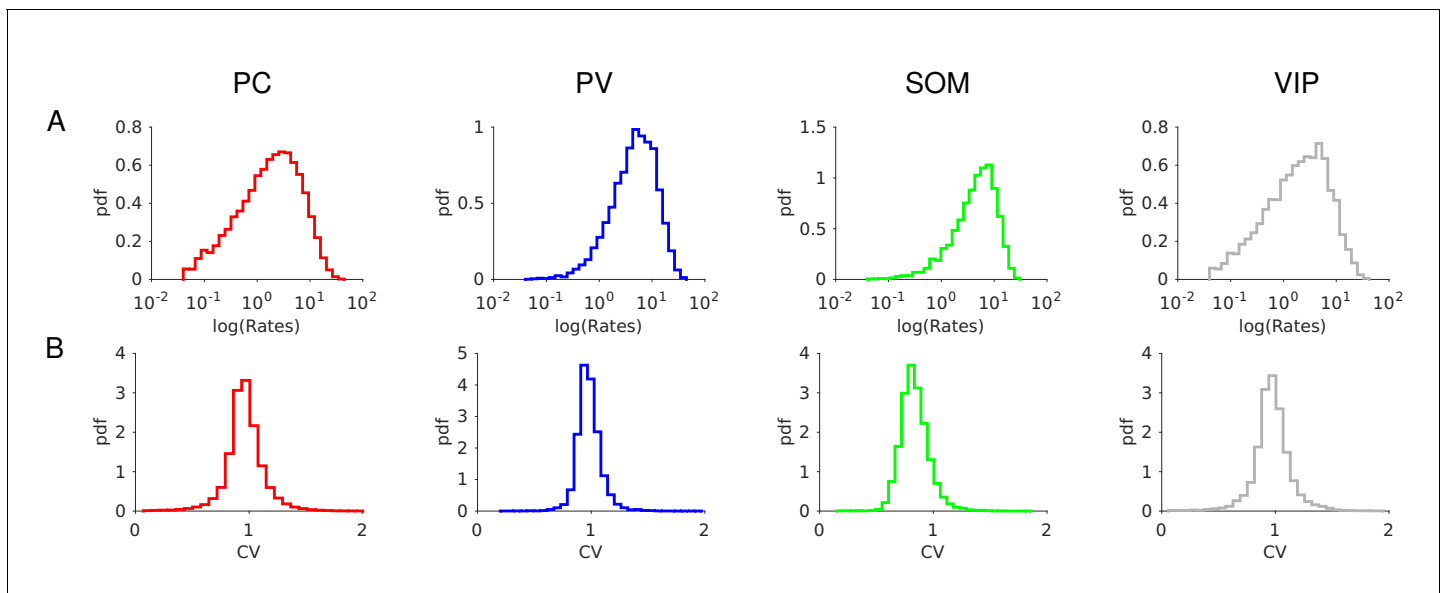


Figure 5—figure supplement 3. Model 1 with $J_{EE} > J_{EE}^*$. Firing statistics at baseline. (A) Distribution of the firing rates (mean: $r_E = 3.3$ Hz, $r_I = 6.5$ Hz, $r_S = 5.9$ Hz, $r_V = 3.5$ Hz). (B) Distribution of CV. Color code as in **Figure 5**. Parameters as in **Figure 5**. Individual rates are averaged over 100s with a threshold at 0.05 Hz. CVs are computed over 30s.

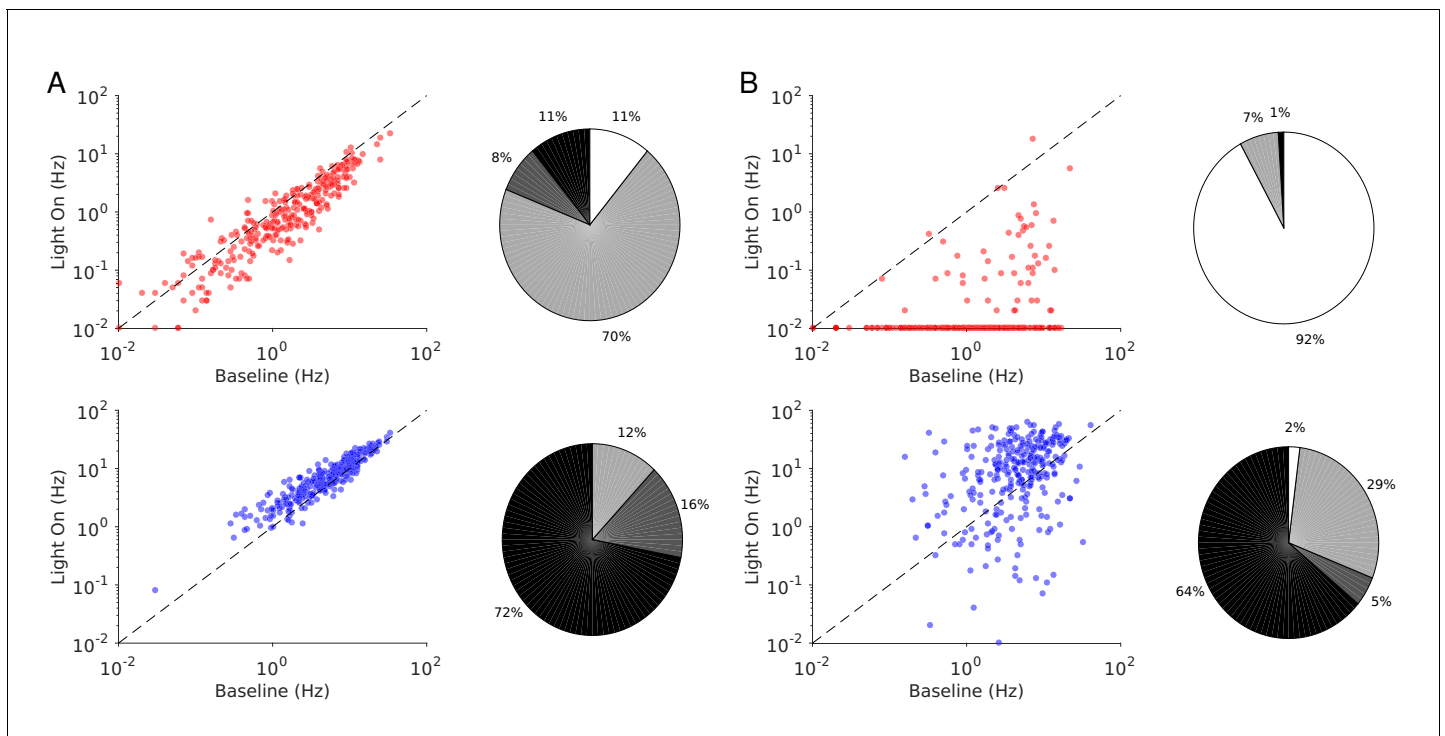


Figure 6. Single neuron firing rates in the PC and PV populations upon PV activation for two values of the light intensity (Model 1 with $J_{EE} > J_{EE}^*$). (A) Single neuron firing rates at baseline vs. at $\Gamma_{opto} = 0.5 \text{ mW.mm}^{-2}$. (B) Same for $\Gamma_{opto} = 1 \text{ mW.mm}^{-2}$. Top: PCs (red). Bottom: PV neurons (blue). Scatter plots of 300 randomly chosen PC and PV neurons. Pie charts for the whole population. The pie charts show the fraction of neurons which increase (black) or decrease (light gray) their activity compared to baseline. Dark gray: Fraction of neurons with relative change smaller than 0.1 Hz. White: fraction of neurons with activity smaller than 0.1 Hz upon PV photostimulation. Firing rates were estimated over 100s. Neurons with rates smaller than 0.01 Hz are plotted at 0.01 Hz. Parameters as in **Figure 5**.

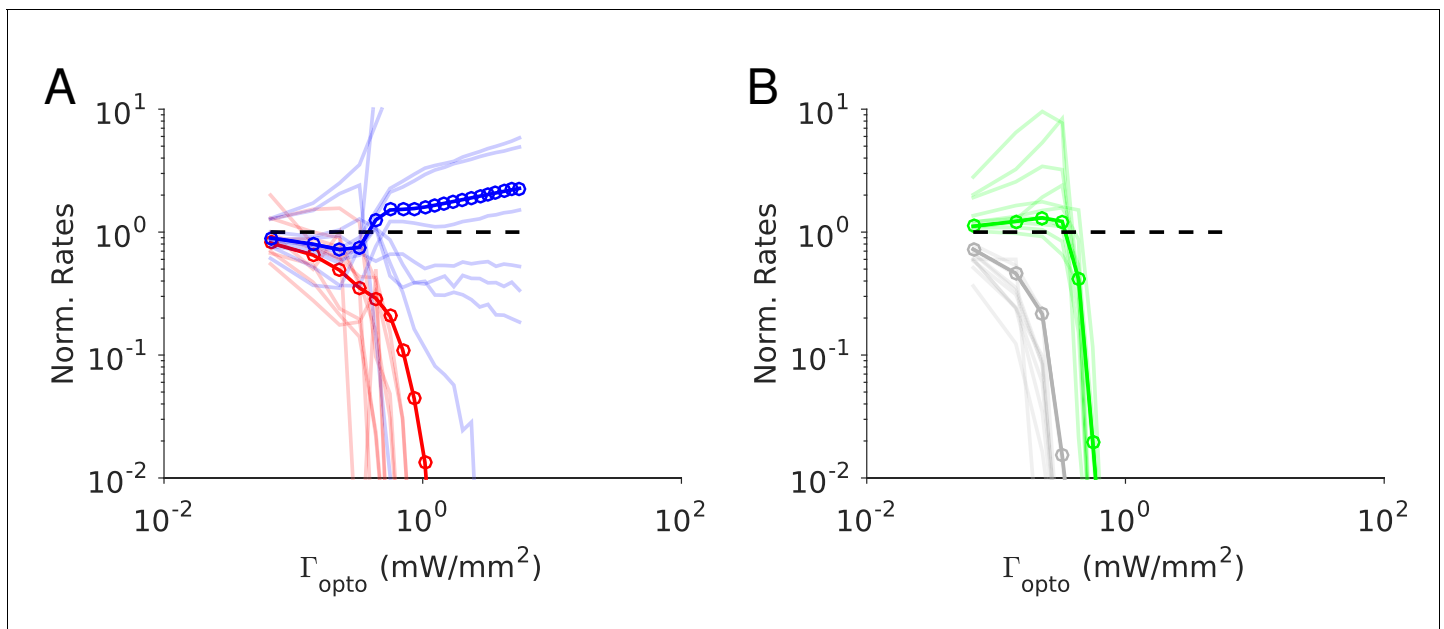


Figure 7. Numerical simulations of Model 1 for $J_{EE} < J_{EE}^*$. Responses of the neurons normalized to baseline vs. the intensity of the laser, Γ_{opto} . (A) Activities of PCs and PV neurons: the PV response is paradoxical. (B) Activities of SOM and VIP neurons. Color code as in **Figure 4**. Thick lines: population averaged responses. Thin lines: responses of 10 neurons in each population. Firing rates were estimated over 100s. Parameters: $K = 500$, $N = 76800$. Other parameters as in **Tables 3–5**. The baseline activities are: $r_E = 4.8$ Hz, $r_I = 11.2$ Hz, $r_S = 7.1$ Hz, $r_V = 5.3$ Hz.

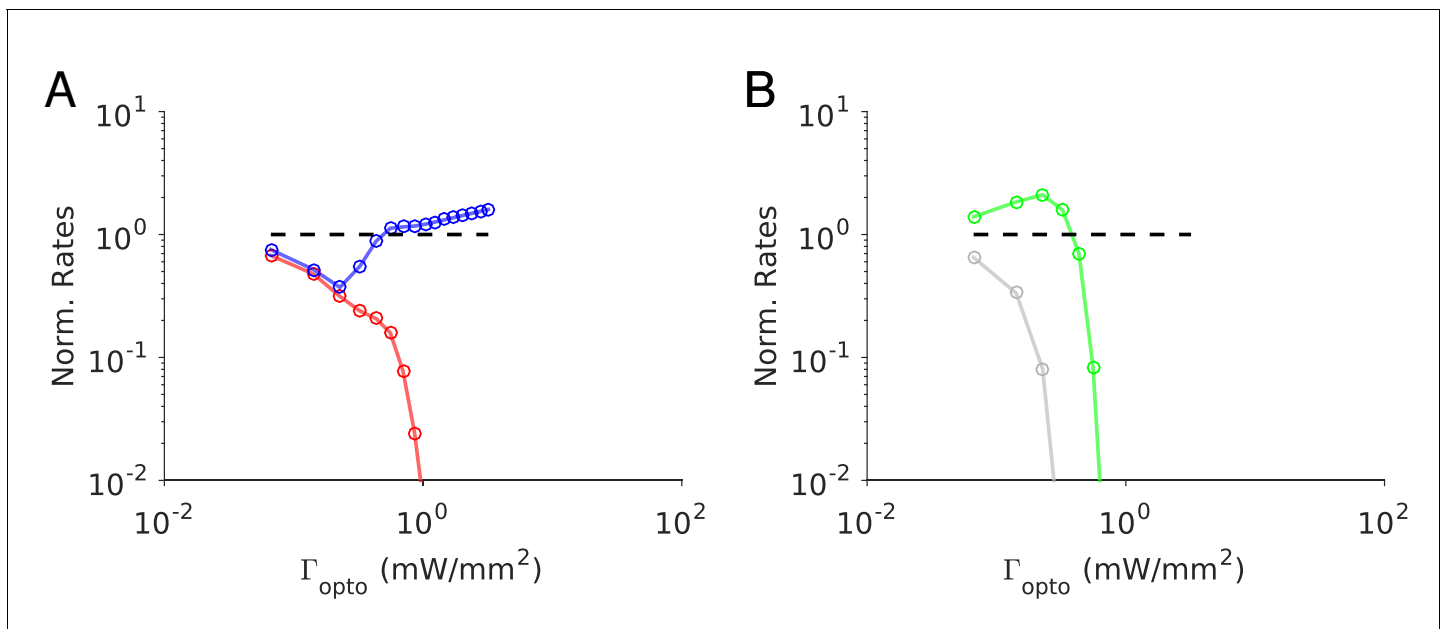


Figure 7—figure supplement 1. Model 1 for $J_{EE} < J_{EE}^*$. Proportionality of the PC and PV activity requires fine-tuning. **(A)** The response of the PV population is paradoxical for small Γ_{opto} and is proportional to the PC response. **(B)** Responses of the SOM and VIP neurons. Baseline firing rates: $r_E = 6.4$ Hz, $r_I = 12.2$ Hz, $r_S = 6.5$ Hz, $r_V = 11.0$ Hz. Color code as in **Figure 7**. Interaction parameters: $J_{EO} = 40 \mu\text{A} \cdot \text{ms} \cdot \text{cm}^{-2}$; $J_{EE} = 20 \mu\text{A} \cdot \text{ms} \cdot \text{cm}^{-2}$; $J_{EI} = 32 \mu\text{A} \cdot \text{ms} \cdot \text{cm}^{-2}$; $J_{ES} = 22 \mu\text{A} \cdot \text{ms} \cdot \text{cm}^{-2}$; $J_{EV} = 0$; $J_{IO} = 31 \mu\text{A} \cdot \text{ms} \cdot \text{cm}^{-2}$; $J_{IE} = 36 \mu\text{A} \cdot \text{ms} \cdot \text{cm}^{-2}$; $J_{II} = 30 \mu\text{A} \cdot \text{ms} \cdot \text{cm}^{-2}$; $J_{IS} = 20 \mu\text{A} \cdot \text{ms} \cdot \text{cm}^{-2}$; $J_{IV} = 0$; $J_{SE} = 26 \mu\text{A} \cdot \text{ms} \cdot \text{cm}^{-2}$; $J_{SI} = 0$; $J_{SS} = 0$; $J_{SV} = 12 \mu\text{A} \cdot \text{ms} \cdot \text{cm}^{-2}$; $J_{VO} = 22 \mu\text{A} \cdot \text{ms} \cdot \text{cm}^{-2}$; $J_{VE} = 28 \mu\text{A} \cdot \text{ms} \cdot \text{cm}^{-2}$; $J_{VI} = 24 \mu\text{A} \cdot \text{ms} \cdot \text{cm}^{-2}$; $J_{VS} = 12 \mu\text{A} \cdot \text{ms} \cdot \text{cm}^{-2}$; $J_{VV} = 0$; . Other parameters as in **Tables 3**.

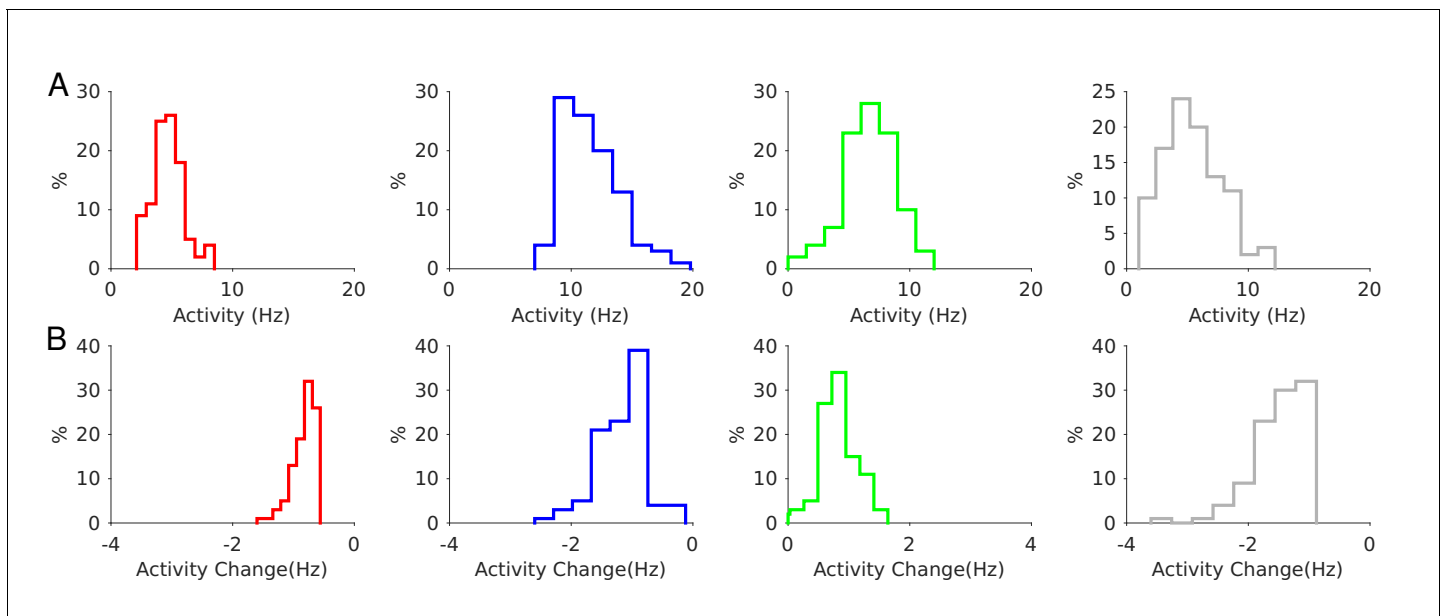


Figure 7—figure supplement 2. Model 1 with $J_{EE} > J_{EE}^*$. Robustness to a change of $\pm 10\%$ in the interaction parameters. (A) Distribution of the population activities. (B) Distribution of the activity changes upon stimulation for $\Gamma_{opto} = 0.07 mW.mm^{-2}$. Rates are averaged over 10s. Color code as in **Figure 7**. Parameters as in **Figure 7**.

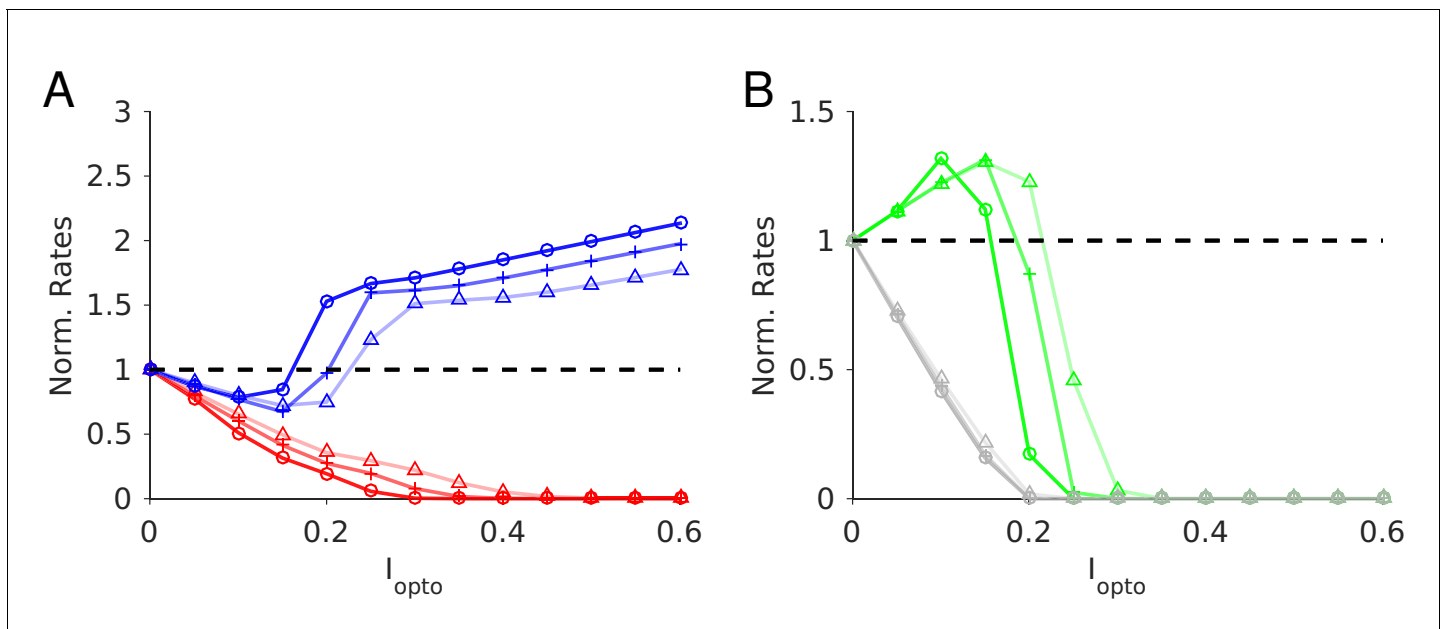


Figure 7—figure supplement 3. Model 1 with $J_{EE} < J_{EE}^*$. Robustness with respect to change in the average connectivity, K . Triangles: $K = 500$; cross: $K = 1000$; circles: $K = 2000$. $N_\alpha = 10000$ neurons per population. Baseline firing rates: $K = 500$: $r_E = 4.7$ Hz, $r_I = 11.2$ Hz, $r_S = 7.1$ Hz, $r_V = 5.2$ Hz; $K = 1000$: $r_E = 4.1$ Hz, $r_I = 10.3$ Hz, $r_S = 7.6$ Hz, $r_V = 4.7$ Hz; $K = 2000$: $r_E = 3.7$ Hz, $r_I = 9.7$ Hz, $r_S = 7.8$ Hz, $r_V = 4.4$ Hz. Rates are averaged over 10s. Color code and parameters as in **Figure 7**.

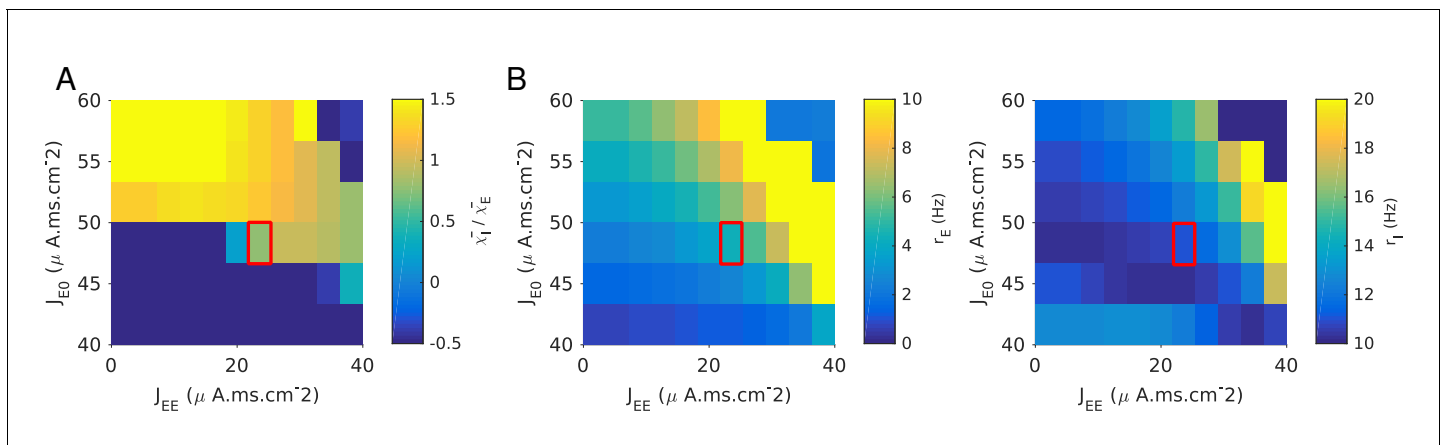


Figure 7—figure supplement 4. Model 1. The response of the PC and PV populations upon stimulation of the latter are proportional only if parameters are fine-tuned. (A) $\bar{\chi}_I/\bar{\chi}_E$ where $\bar{\chi}_A = \left(\frac{A_{light\ on}}{r_A} - 1\right)/\Gamma_{opto}$ estimated for $\Gamma_{opto} = 0.5mW.mm^{-2}$. (B) Red square indicates the region of the parameter space for which the ratio of the PC and PV slopes 1 ± 0.3 and activities are reasonable ($r_E < 5$ Hz, $5Hz < r_I < 10$ Hz). Parameters as in Figure 5. $K = 500$.

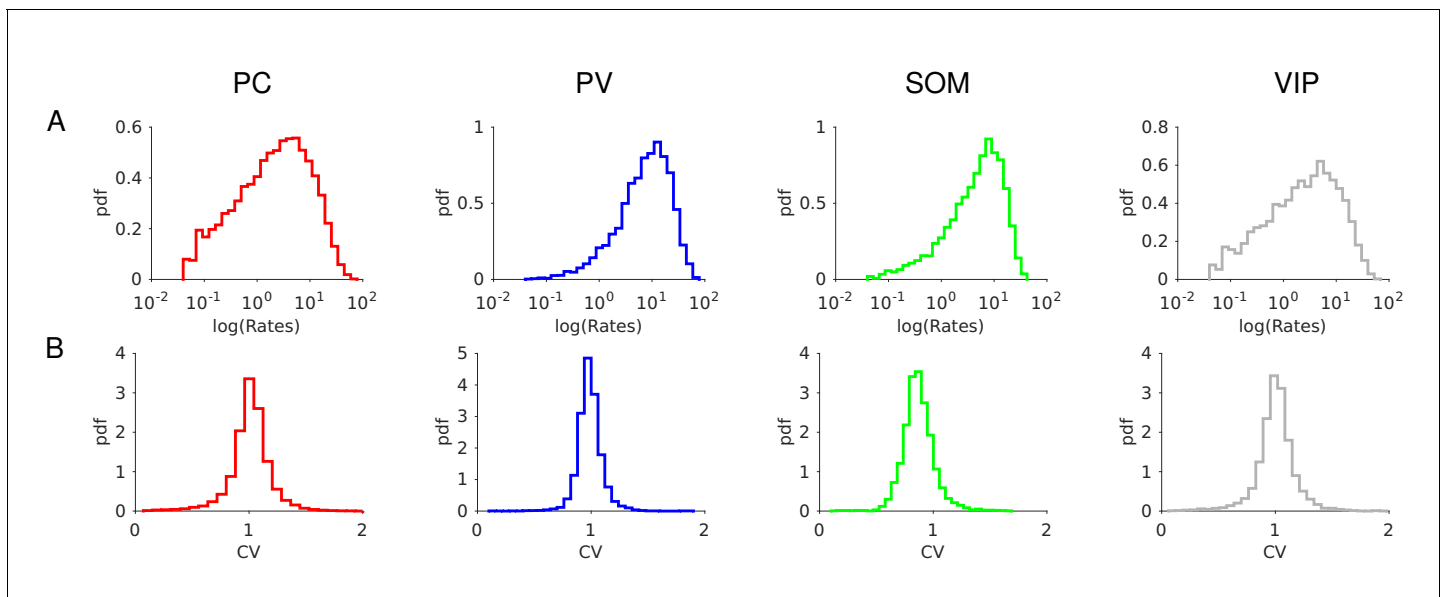


Figure 7—figure supplement 5. Model 1 with $J_{EE} < J_{EE}^*$. Firing statistics at baseline. **(A)** Distribution of the firing rates (mean: rE = 4.8 Hz, rI = 11.2 Hz, rS = 7.1 Hz, rV = 5.3 Hz). **(B)** Distribution of CV. Individual rates are average over 100s with a threshold at 0.05Hz. CVs are computed over 30s. Color code as in **Figure 7**. Parameters as in **Figure 7**.

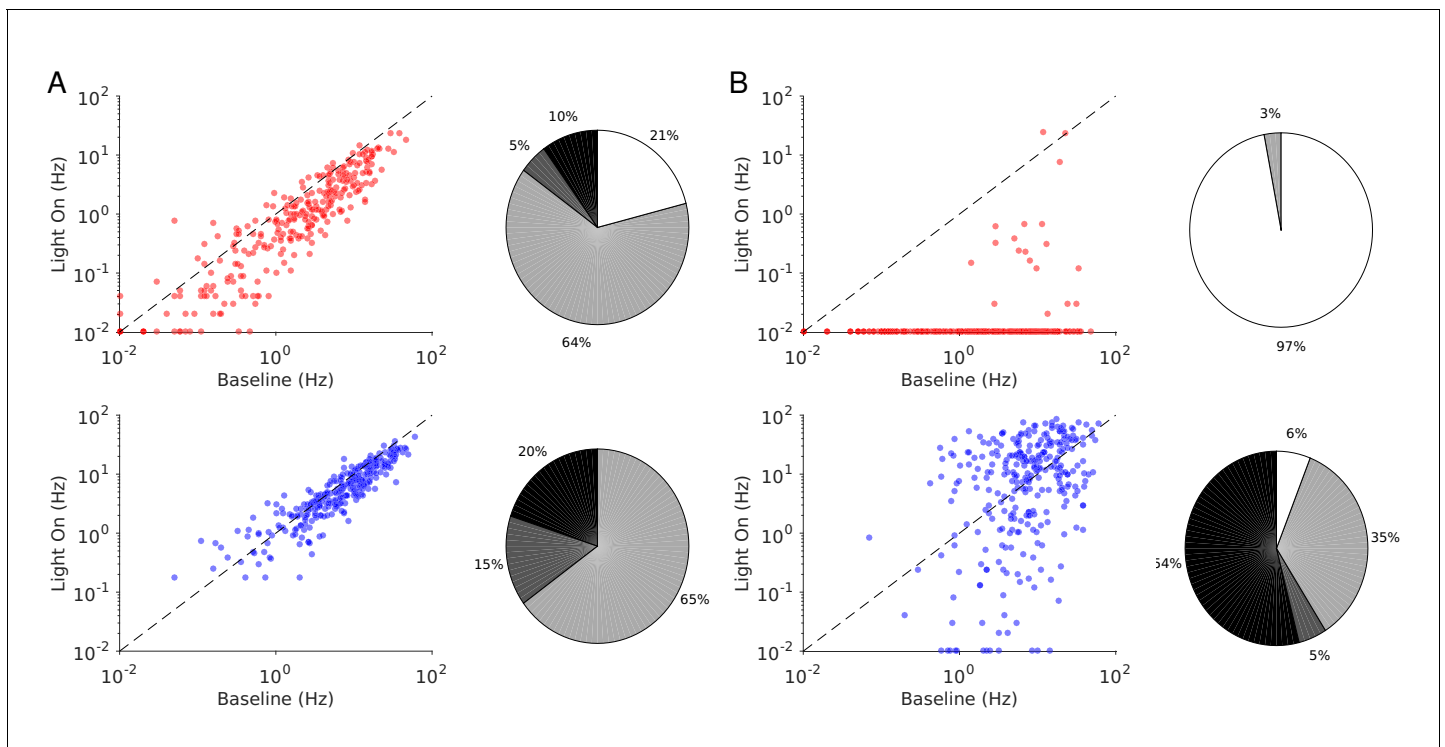


Figure 8. Single neuron firing rates in the PC and PV populations upon PV activation for two values of the light intensity (Model 1 with $J_{EE} < J_{EE}^*$). (A) Single neuron firing rates at baseline vs. at $\Gamma_{opto} = 0.5 mW/mm^2$. (B) Same for $\Gamma_{opto} = 1 mW/mm^2$. Top: PCs. Bottom: PV neurons. Scatter plots of 300 randomly chosen PC and PV neurons. Pie charts for the whole population. Firing rates were estimated over 100s simulation time. Neurons with rates smaller than 0.01Hz are plotted at 0.01Hz. Color code as in **Figure 6**. Parameters as in **Figure 7**.

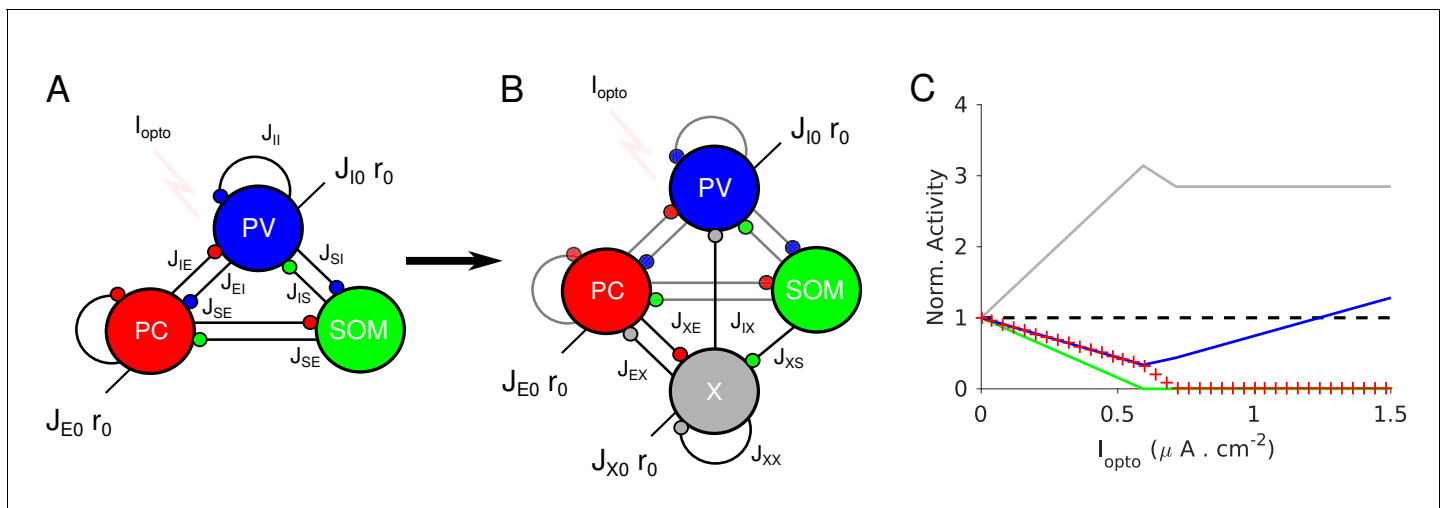


Figure 9. Network models with proportional change in the PC and PV activities upon photostimulation of the PV population. (A) A three-population network consisting of PCs, PV and SOM neurons. SOM neurons only receive projections from the PC and PV populations. (B) Model 2 consists of four populations: PC, PV, SOM and an unidentified inhibitory population, X. The population X projects to the PC, the PV population and to itself. The PC population projects to X. (C) Population activities normalized to baseline vs. I_{opto} in the large N , K limit. PC and PV populations decrease their activity with I_{opto} in a proportional manner. Parameters as in **Tables 6–7**. Baseline firing rates are: $r_E = 3.0$ Hz, $r_I = 6.7$ Hz, $r_S = 6.4$ Hz, $r_X = 3.8$ Hz.

$$\chi_{II} = \frac{1}{J_{SE} \Delta} \left[J_{XX} \text{X} \times \text{PC} \begin{matrix} \xrightarrow{J_{SE}} \text{SOM} \\ \xleftarrow{J_{ES}} \end{matrix} - \text{PC} \begin{matrix} \xrightarrow{J_{SE}} \text{SOM} \\ \xleftarrow{J_{EX}} \text{X} \end{matrix} \xrightarrow{J_{XS}} \text{SOM} \right]$$

Figure 9—figure supplement 1. Model 2. Graphical representation of χ_{II} (large N, K limit). Note : $\chi_{EI} = \frac{J_{SI}}{J_{SE}} \chi_{II}$.

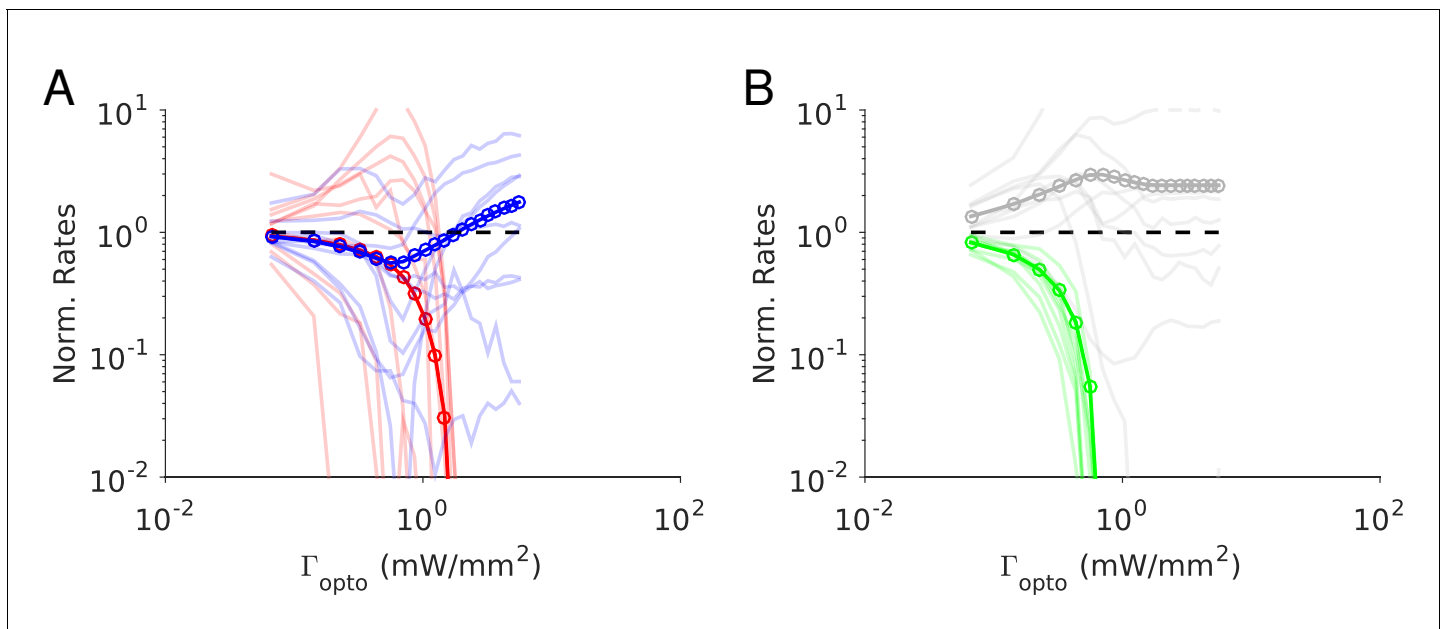


Figure 10. Numerical simulations of Model 2. Responses of the neurons normalized to baseline vs. the intensity of the laser, Γ_{opto} . (A) Activities of PCs and PV neurons: for small Γ_{opto} , the PV response is paradoxical and the suppression of the PC and PV population activities relative to baseline are the same. (B) Activities of SOM and X neurons. Color code as in **Figure 9**. Thick lines: population averaged responses. Thin lines: responses of 10 neurons randomly chosen in each population. Firing rates were estimated over 100s. Parameters: $K = 500$, $N = 76800$. Other parameters as in **Tables 6–7**. The baseline activities are: $r_E = 4.2$ Hz, $r_I = 6.8$ Hz, $r_S = 7.0$ Hz, $r_X = 3.9$ Hz.

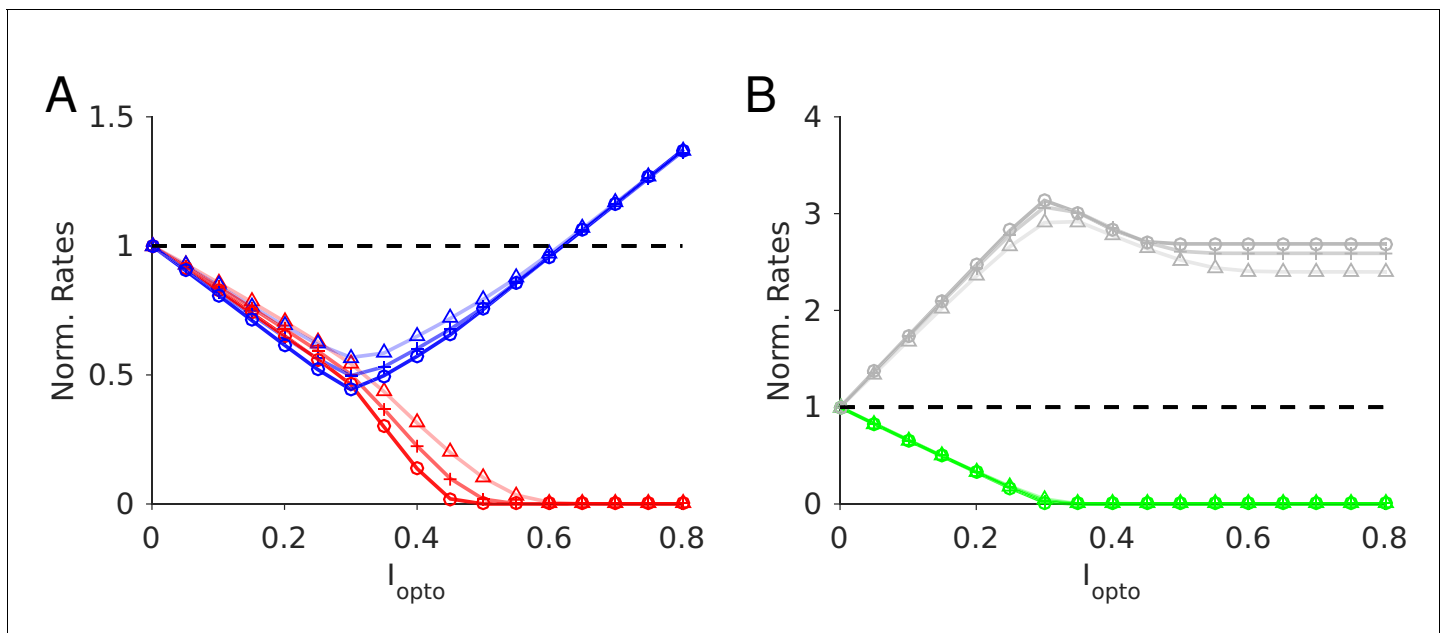


Figure 10—figure supplement 1. Model 2. Robustness with respect to change in the average connectivity, K . Triangles: $K = 500$; cross: $K = 1000$; circles: $K = 2000$. $N_a = 10000$ neurons per population. Color code and parameters as in **Figure 10**. Baseline firing rates: $K = 500$: $r_E = 4.2$ Hz, $r_I = 7.0$ Hz, $r_S = 7.0$ Hz, $r_X = 4.0$ Hz; $K = 1000$: $r_E = 4.0$ Hz, $r_I = 6.8$ Hz, $r_S = 6.8$ Hz, $r_X = 3.8$ Hz; $K = 2000$: $r_E = 3.7$ Hz, $r_I = 6.8$ Hz, $r_S = 6.7$ Hz, $r_X = 3.8$. Rates are averaged over 10s.

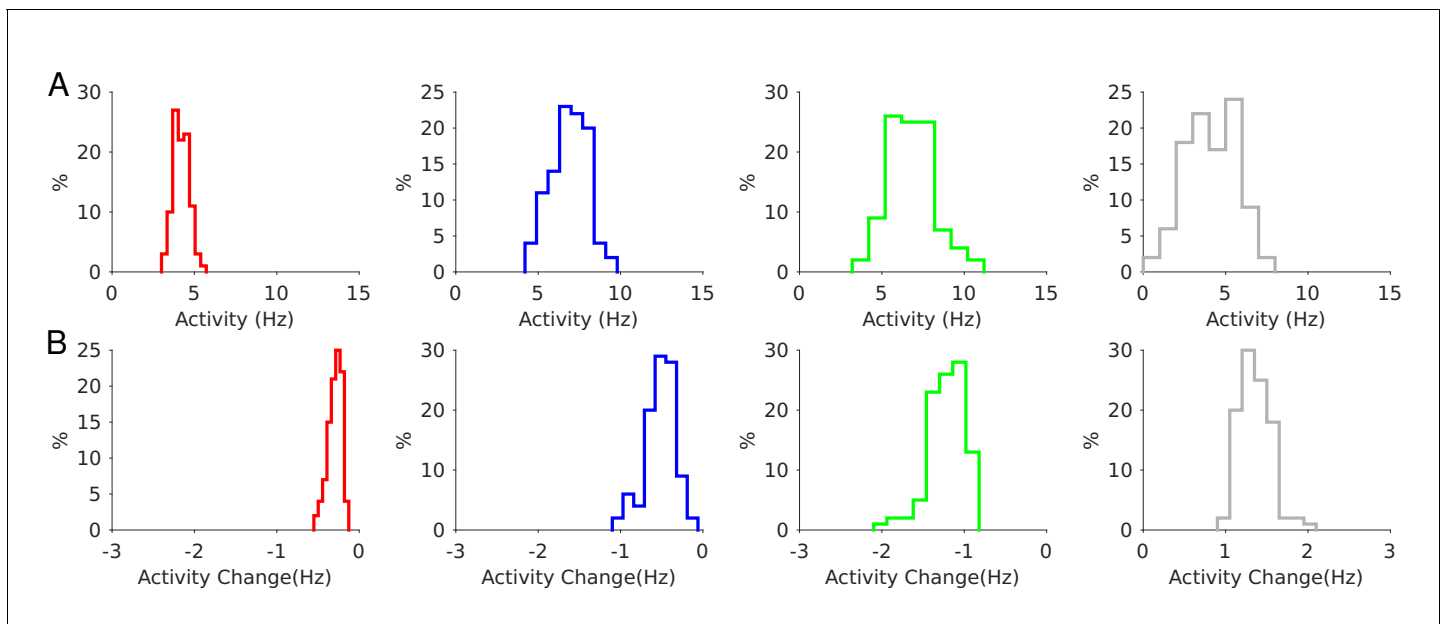


Figure 10—figure supplement 2. Model 2. Robustness to a change of $\pm 10\%$ in the interaction parameters. (A) Distribution of the population activities. (B) Distribution of the activity changes upon stimulation for $\Gamma_{opto} = 0.07 \text{ mW.mm}^{-2}$. Rates are averaged over 10s. Color code as in **Figure 10**.

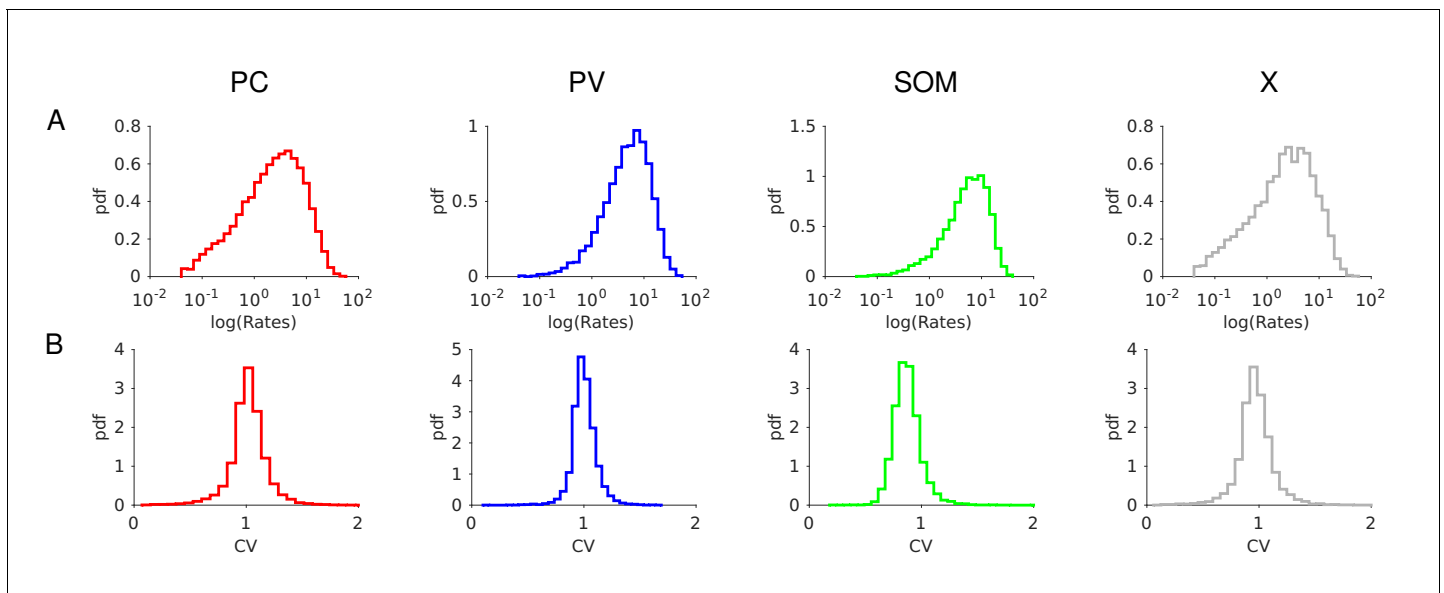


Figure 10—figure supplement 3. Model 2. Firing statistics at baseline. (A) Distribution of the firing rates (mean: $r_E = 4.5$ Hz, $r_I = 10.6$ Hz, $r_S = 7.2$ Hz, $r_V = 4.9$ Hz). (B) Distribution of CV. Individual rates are average over 100s with a threshold at 0.05Hz. CVs are computed over 30s. Color code and parameters as in **Figure 10**.

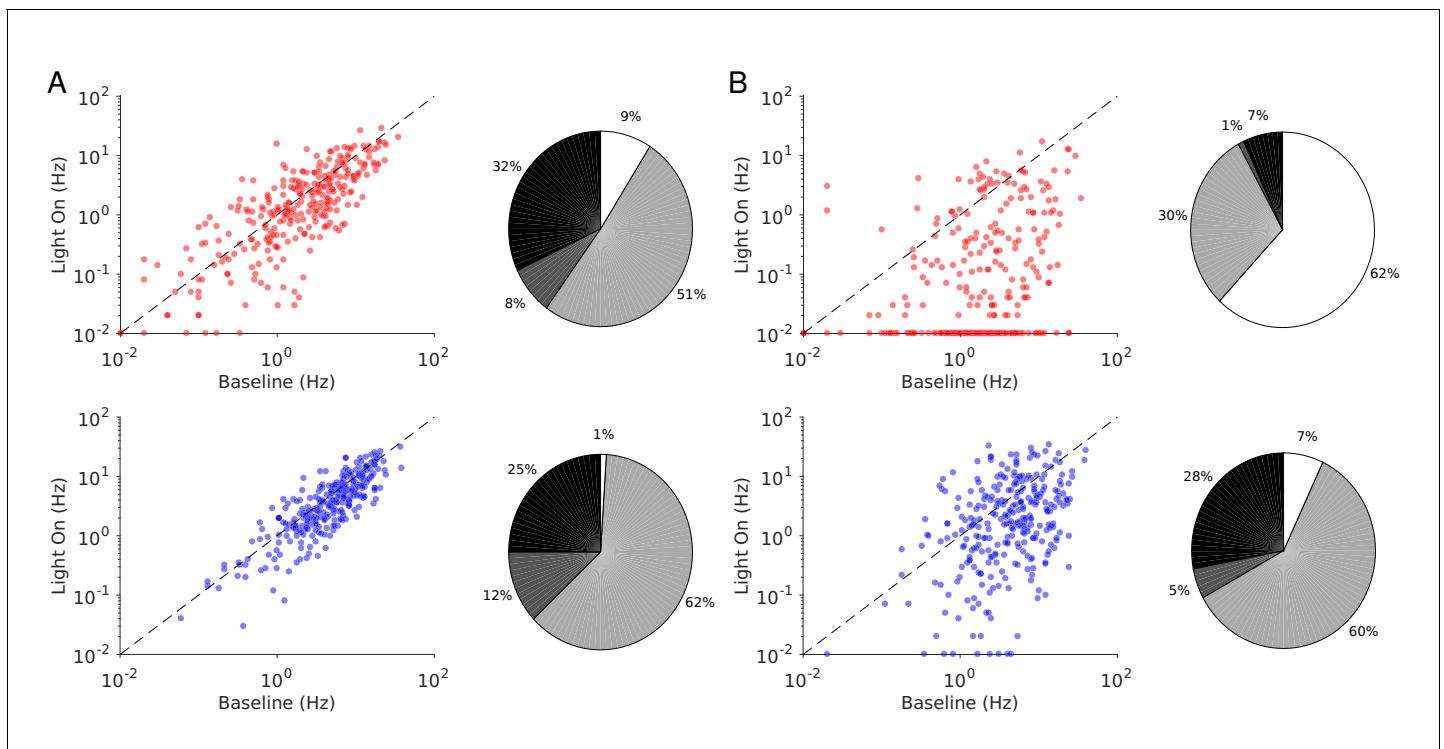


Figure 11. Single neuron firing rates in the PC and PV populations upon PV activation for two values of the light intensity (Model 2). **(A)** Single neuron firing rates at baseline vs. at $\Gamma_{opto} = 0.5 \text{ mW} \cdot \text{mm}^{-2}$. **(B)** Same for $\Gamma_{opto} = 1 \text{ mW} \cdot \text{mm}^{-2}$. Top: PCs. Bottom: PV neurons. Scatter plots of 300 randomly chosen PC and PV neurons. Pie charts for the whole population. Firing rates were estimated over 100s. Neurons with rates smaller than 0.01Hz are plotted at 0.01Hz. Color code as in **Figure 6**. Parameters as in **Figure 10**.

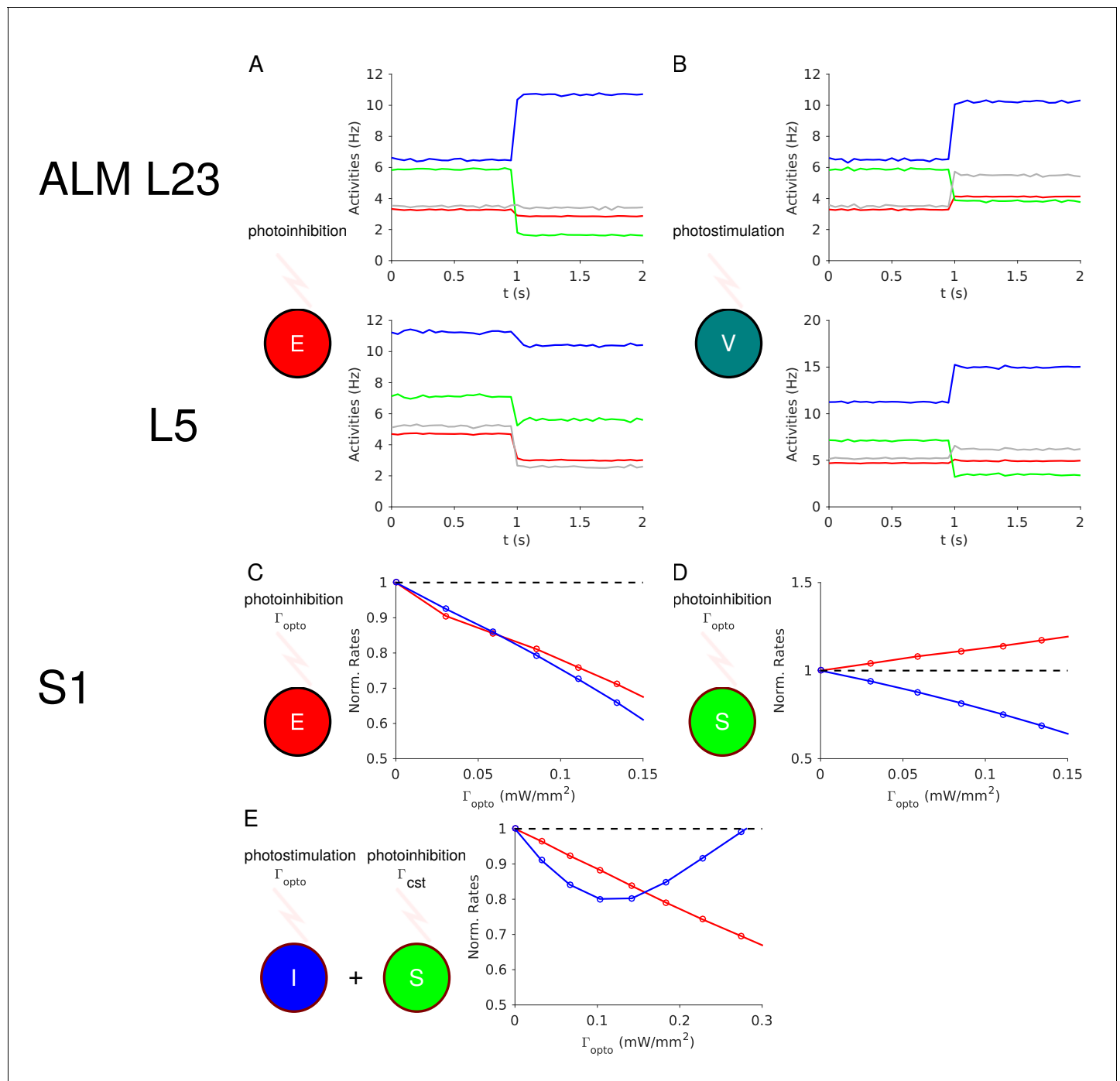


Figure 12. Predictions of the theory. (A) In ALM layer 2/3, the activity of the PV population decreases upon photoinhibition of the PCs. (B) In ALM layer 2/3, photostimulation of VIP neurons increases the activity of the PV population. (C) In S1, PV and PC activity decrease proportionally upon photoinhibition of the latter. (D) In S1, the PC and PV responses are not proportional upon photoinhibition of the SOM population. (E) In S1, upon photostimulation of PV neurons and photoinhibition of the SOM population with a constant input, the PV response is paradoxical but PC and PV responses are no longer proportional.